ELSEVIER

Journal of Alloys and Compounds 408–412 (2006) 294–300

Journal of ALLOYS AND COMPOUNDS

www.elsevier.com/locate/jallcom

Development of Mg-containing $MmNi_5$-based alloys for low-cost and high-power Ni–MH battery

Tetsuya Ozaki [a,*], Hua-Bin Yang [a], Tsutomu Iwaki [a], Shigeo Tanase [a], Tetsuo Sakai [a], Hiroshi Fukunaga [b], Nobuaki Matsumoto [b], Yoshihiro Katayama [c], Toshiki Tanaka [c], Tomonori Kishimoto [c], Minoru Kuzuhara [c]

[a] *National Institute of Advanced Industrial Science and Technology (AIST) Kansai, 1-8-31, Midorigaoka, Ikeda, Osaka 563-8567, Japan*
[b] *Hitachi Maxell Ltd., 1-1-88, Ushitora, Ibaraki, Osaka 567-8567, Japan*
[c] *GS Yuasa Corporation, 2-3-21, Kosobe-cho, Takatsuki, Osaka 569-1115, Japan*

Available online 1 July 2005

Abstract

Mg-added $MmNi_5$-based alloy with low Co content was developed for nickel/metal hydride (Ni–MH) battery, satisfying low-cost, high-power, and long-term endurance, simultaneously. High rate capability and cycle life of the alloy was improved by controlling alloy composition and alloy preparation-conditions. Alloy with overstoichiometric composition (B/A = 5.2) showed higher rate capability than stoichiometric alloy (B/A = 5.0), in spite of its lower theoretical capacity.

AAA-sized sealed battery using the developed alloy ($Mm_{0.96}Mg_{0.04}Ni_{4.2}Co_{0.3}Mn_{0.4}Al_{0.3}$) showed comparable high rate capability and cycle life to that using the conventional alloy ($MmNi_{4.0}Co_{0.65}Mn_{0.3}Al_{0.28}$). Hybrid electric vehicle (HEV) mode cycle test was then carried out at 45 °C using short-D-sized sealed cell (diameter: 32 mm, height: 44 mm). Both capacity and power output of the cell remained more than 80% of the initial values even after 25,000 cycles (corresponding to 100,000 km). It is concluded that the developed alloy with low cost would be used for HEV application, satisfying both high-power output and long cycle life.

Keywords: Nickel/metal hydride battery; Hydrogen storage alloys; Negative electrode; Hybrid electric vehicle; Low-cobalt alloy

1. Introduction

Research and development on nickel/metal hydride (Ni–MH) battery is now focused on application to hybrid electric vehicle (HEV) [1–3]. It is eagerly hoped to improve power and reduce cost of Ni–MH battery. Conventional AB_5-type Mm–Ni–Co–Mn–Al (Mm: mischmetal) alloys have been used for negative electrode of Ni–MH battery. It is well known that Co is an essential element in the electrode alloys for suppression of cycle degradation [4,5]. Although the Co content in them is only about 10%, its cost accounts for half of the total alloy cost. Reduction in Co content is an important issue for cost reduction in the alloy for Ni–MH battery. Various low-cobalt and cobalt-free alloys have been developed [6–14]. Sakai et al. reported addition of small amount of Zr on $LaNi_5$ alloy remarkably improved the cycle life of alloy electrode [6]. Hasagawa et al. reported that cobalt could be substituted with Fe keeping relatively long cycle life [7]. Addition of Si [8] and Sn [9] instead of Co also have been reported to be effective for improvement in the cycle life. Improvement in cycle life by controlling stoichiometric composition has been reported [10,11]. At present, practical low-cobalt or cobalt-free alloys have not been used in the practical battery.

In recent years, there have been several impressive works on La–Mg–Ni alloys and related systems [15–19]. Kadir et al. have developed AB_2C_9 (A: rare earths, Ca; B: Mg, Ca; C: Ni)-type alloys with stacking structure consisting of AB_5 and AB_2 units [15,16]. Kohno et al. reported that $La_5Mg_2Ni_{23}$ with B/A ratio of 3.3 showed 410 mAh/g of discharge capacity, which was about 1.3 times of those of AB_5-type alloys [17].

* Corresponding author.
E-mail address: ozaki-tetsuya@aist.go.jp (T. Ozaki).

0925-8388/$ – see front matter © 2005 Elsevier B.V. All rights reserved.
doi:10.1016/j.jallcom.2005.04.183

Maeda et al. reported that addition of small amount of Mg was effective to improve the cycle life of low-cobalt AB_5-type alloy [18]. Recently, it has been shown that the Co content was successfully reduced to half of the conventional alloy ($MmNi_{4.0}Co_{0.65}Mn_{0.3}Al_{0.28}$) by the addition of small amount of Mg [19].

The aim of this work is to develop practical Mg-added Mm-based alloys with low Co content, which could satisfy high rate capability and long cycle life, and to demonstrate their performance in AAA-sized sealed cell, and finally in short-D-sized sealed cell using the HEV mode cycle pattern.

2. Experimental details

2.1. Preparation and characterization of alloy samples

The Mg-added AB_5-type alloys, $Mm_{1-x}Mg_xNi_{4.5-y}Co_yMn_{0.4}Al_{0.3}$ (Mm comprises 80 at.% La, 10 at.% Ce, 6 at.% Pr, and 4 at.% Nd; $x = 0.03$, 0.04, 0.05, and 0.06; $y = 0.3$ and 0.325), were prepared by induction melting on 10 kg-batch scale and then annealed at 1000–1100 °C. Mg-added alloys with different stoichiometric ratio, $Mm_{0.96}Mg_{0.04}Ni_xCo_{0.3}Mn_{0.4}Al_{0.3}$ ($x = 4.0$ and 4.1) and alloy with similar composition to standard commercial one, $MmNi_{4.0}Co_{0.65}Mn_{0.3}Al_{0.28}$ (hereinafter called "conventional alloy") were also prepared. The alloy ingots were ground into powders with average particle sizes of 20 μm, which were determined by a Shimadzu SK-LMS PRO-7000S laser particle size analyzer. The crystal structure and lattice parameters were determined by X-ray diffraction (XRD) measurement using a Rigaku Rint 2000 V with Cu Kα radiation. Pressure composition isotherms (PCTs) were determined with an automatic Sieverts-type apparatus at 80 °C.

2.2. Assembly of test cell

The electrochemical capacity, high rate capability, and cycle life of the alloys were examined in test cells using a 30% (w/w) KOH + 30 g/L LiOH electrolyte at 25 °C. The alloy electrodes for test cells were prepared as follows. Test alloys of 95 wt.% were well mixed with 5 wt.% Ni powder (Inco 255) together with 0.2 wt.% poly(vinyl alcohol) aqueous solution (Kishida Chemical Co. Ltd.) as a binder. This mixture was pasted into a nickel-foam, then pressed to form a plate with thickness of about 0.26 mm by roll press. Sintered $NiOOH/Ni(OH)_2$ plates (Yuasa Corporation) were used as positive electrodes. Each alloy electrodes was placed in the central compartment, and two pieces of sintered Ni electrodes of the same size were placed on either side. A sulfonated polypropylene non-woven separator (Japan Vilene Co. Ltd.) was used to separate the positive and negative electrodes.

During the formation process, each cell was charged at the 0.2*C* rate (60 mA/g) for 6 h followed by 30 min rest, and then discharged at the 0.3*C* rate (90 mA/g) to 1 V cutoff, where $(1/n)C$ rate means charging or discharging rate that charges or discharges the cell in n h. To make it completely activated, the cell was charged and discharged for 15 cycles. The rate capability was evaluated by charging at the 0.2*C* rate for 6 h and discharging at the 0.2, 1, 5, and 10*C* rate with cutoff voltage of 1.0, 1.0, 0.6, and 0.5 V, respectively. The cycle performance was examined by charging at the 1*C* rate for 1.2 h and discharging at the same rate to 1 V. Cycle life was defined as the cycle number at which discharge capacity fell below 150 mAh/g. Transmission electron microscope (TEM) observation was carried out for the alloys after 150 cycles of the cycle test. All the charge and discharge tests were performed using a computer-controlled charge/discharge system (Keisokuki center: BLS2500).

2.3. Assembly of AAA- and short-D-sized sealed cells

For more practical evaluation of the alloy electrodes, AAA-sized cylindrical sealed cells (diameter: 10.5 mm, height: 43 mm) were prepared. The negative electrodes for AAA-sized cells were prepared as follows. The alloy powder, the nickel powder, carboxymethyl cellulose (CMC) (Daiichi Kogyo), and styrene butadiene rubber (SBR) (JSR Corporation) were mixed well in the weight ratio of 100:2:0.3:1 together with water. This mixture was pasted into punched metal sheet, and pressed to form a plate with thickness of 0.16 mm by roll press. The plate was cut into the size of 36 mm × 100 mm and used as an electrode. The positive electrode with thickness of 0.23 mm was prepared using CoOOH-coated $Ni(OH)_2$ powder as an active material and Ni-coated three-dimensional steel sheet [20,21] as a substrate, and was cut into the size of 36 mm × 80 mm. The positive and negative electrodes were spirally wound together with the sulphonated polypropylene separator. The cell bundle was inserted into a can. After electrolyte (30%, w/w, KOH + 17g/L LiOH) was added, cover plate was welded to terminal of the positive electrode, and sealed. High rate capability of the AAA-sized cells was examined by charging at the 1*C* rate (0.4 A) to 5 mV of negative delta voltage ($-\Delta$ V), followed by rest for 1 h, and discharging at the 25*C* rate (10.0 A) to 0.6 V cutoff. The cycle life was examined by repeating charge–discharge pattern consisting of charging at the 2*C* rate (0.8 A) to 5 mV of $-\Delta$ V, rest for 15 min, and discharging at the 2*C* rate (0.8 A) to 1.0 V cutoff. High rate discharging and cycle tests were carried out at 25 °C.

Short-D-sized sealed cell (diameter: 32 mm, height: 44 mm, rated capacity: 5 Ah) [21] with the same diameter and the half height as D-sized cell was prepared. HEV mode cycle test was conducted according to test procedure of Ni–MH battery for HEV established in Japan Electric Vehicle Standard (JEVS) by Japan Automobile Research Institute (JARI) [22]. HEV mode cycle test was performed by repeating cycle pattern for 360 s (Fig. 1), in which maximum charging and discharging rates were the 11 and 7*C*, respectively. Discharge capacity at 0.2*C* and power output were measured every 3000 cycles.

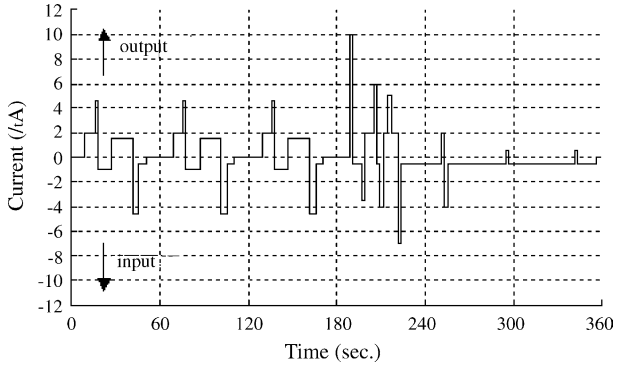

Fig. 1. Relationship between time and current in HEV mode cycle pattern [22].

3. Results and discussion

3.1. Effect of Mg and Co content on electrode properties

All the developed alloys ($Mm_{1-x}Mg_xNi_{4.5-y}Co_yMn_{0.4}Al_{0.3}$, $x = 0.03$, 0.04, 0.05, and 0.06; $y = 0.3$ and 0.325) were crystallized in hexagonal $CaCu_5$-type structure (space group *P*6/*mmm*). Their lattice parameters and PCT results were not largely dependent on the Mg and Co content (Table 1). The plateau pressure and the H/M values of the alloys were in the range of 0.14–0.17 MPa and 0.64–0.68, respectively.

Fig. 2 shows the high rate capabilities of test cells using the developed Mg-added alloys ($Mm_{1-x}Mg_xNi_{4.2}Co_{0.3}Mn_{0.4}Al_{0.3}$, $x = 0.03$, 0.04, and 0.05) compared with that using the conventional alloy ($MmNi_{4.0}Co_{0.65}Mn_{0.3}Al_{0.28}$). At the 10*C* rate, discharge capacities of the developed alloys were in the range of 160–180 mAh/g, which were much higher than that of the conventional alloy, 110 mAh/g.

Fig. 3 shows cyclic behavior of the developed alloys compared with the conventional alloy. Cycle life, which was defined as the cycle number at which discharge capacity fell below 150 mAh/g of the alloys, increased from 188 to 291 cycles with increasing the Mg content. The alloy with $x = 0.05$ showed longer cycle life than that of the conventional alloy, 251 cycles.

Fig. 4 shows dependence of discharge capacity at the 10*C* rate and cycle life on the Mg content for the $Mm_{1-x}Mg_xNi_{4.2}Co_{0.3}Mn_{0.4}Al_{0.3}$ alloys prepared on 1 kg-[19] and 10 kg-batch scale (this work). High rate capability of the alloys was remarkably improved by scaling up to 10 kg batch. Discharge capacity of the alloy with $x = 0.04$ increased from 80 to 170 mAh/g. Previously, it was observed for the alloys prepared on 1 kg-batch scale that the increase in the Mg content caused the decrease in high rate capability [19]. However, this kind of behavior was not observed for

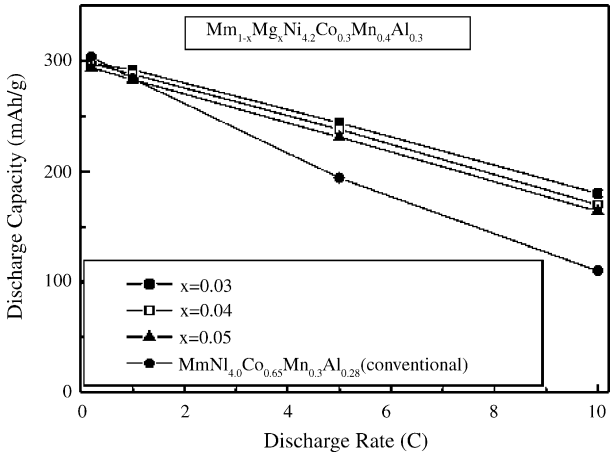

Fig. 2. Discharge capacity vs. discharge rate of test cells using $Mm_{1-x}Mg_xNi_{4.2}Co_{0.3}Mn_{0.4}Al_{0.3}$ ($x = 0.03$, 0.04, and 0.05) alloy and the conventional alloy ($MmNi_{4.0}Co_{0.65}Mn_{0.3}Al_{0.28}$) (Mm comprises 80 at.% La, 10 at.% Ce, 6 at.% Pr, and 4 at.% Nd) electrodes at 25 °C.

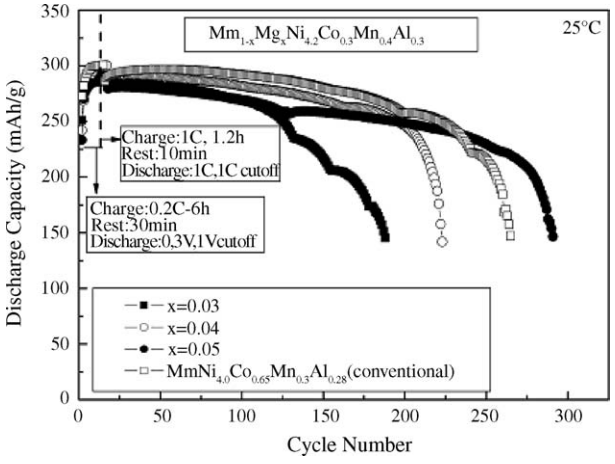

Fig. 3. Discharge capacity vs. cycle number in 1*C*/1*C* cycle test of test cells using $Mm_{1-x}Mg_xNi_{4.2}Co_{0.3}Mn_{0.4}Al_{0.3}$ ($x = 0.03$, 0.04, and 0.05) alloy and the conventional alloy ($MmNi_{4.0}Co_{0.65}Mn_{0.3}Al_{0.28}$) electrodes at 25 °C.

Table 1
Lattice parameters and PCT results (80 °C) for $Mm_{1-x}Mg_xNi_{4.5-y}Co_yMn_{0.4}Al_{0.3}$ ($x = 0.03$, 0.04, 0.05, and 0.06; $y = 0.3$ and 0.325) alloys

x	*y*	Composition	Lattice constants		Unit cell volume (Å^3)	Plateau pressure (MPa)	H/M
			a (Å)	*c* (Å)			
0.03	0.3	$Mm_{0.97}Mg_{0.03}Ni_{4.2}Co_{0.3}Mn_{0.4}Al_{0.3}$	5.034	4.059	89.08	0.14	0.68
0.04	0.3	$Mm_{0.96}Mg_{0.04}Ni_{4.2}Co_{0.3}Mn_{0.4}Al_{0.3}$	5.034	4.061	89.14	0.15	0.64
0.05	0.3	$Mm_{0.95}Mg_{0.05}Ni_{4.2}Co_{0.3}Mn_{0.4}Al_{0.3}$	5.030	4.055	88.84	0.17	0.64
0.04	0.325	$Mm_{0.96}Mg_{0.04}Ni_{4.175}Co_{0.325}Mn_{0.4}Al_{0.3}$	5.034	4.058	89.05	0.16	0.67
0.05	0.325	$Mm_{0.95}Mg_{0.05}Ni_{4.175}Co_{0.325}Mn_{0.4}Al_{0.3}$	5.029	4.061	88.94	0.15	0.65
0.06	0.325	$Mm_{0.95}Mg_{0.06}Ni_{4.175}Co_{0.325}Mn_{0.4}Al_{0.3}$	5.026	4.056	88.74	0.17	0.64

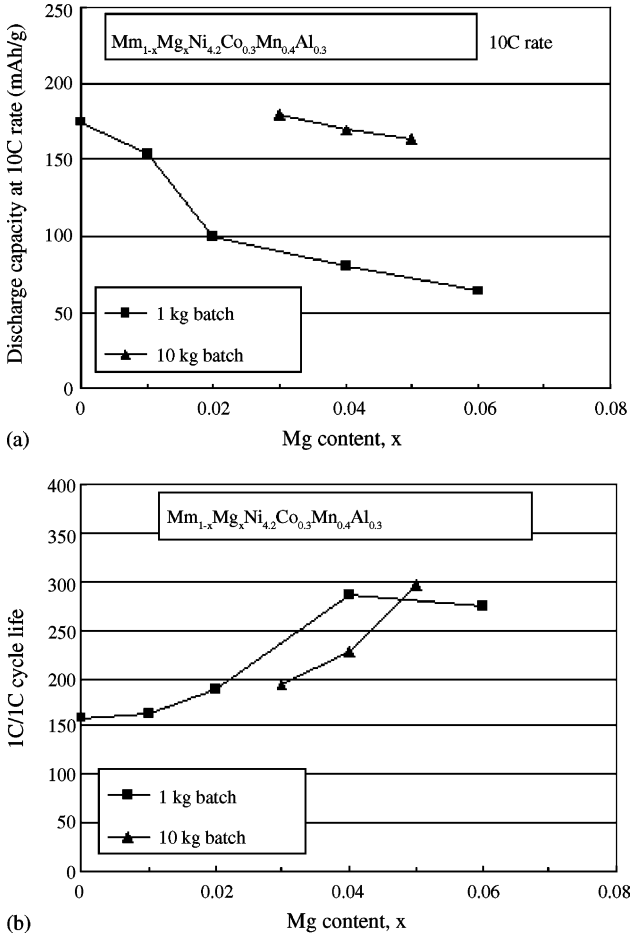

Fig. 4. Dependence of (a) discharge capacity at 10*C* rate and (b) 1*C*/1*C* cycle life on Mg content for test cells using $Mm_{1-x}Mg_xNi_{4.2}Co_{0.3}Mn_{0.4}Al_{0.3}$ ($x = 0.03$, 0.04, and 0.05) alloys prepared on 1 kg- and 10 kg-batch scale.

the alloys prepared on 10 kg-batch scale. Though the reason is not clear at present, it may be ascribed to improvement in homogeneity of the alloys. While targeted Mg content of $Mm_{0.96}Mg_{0.04}Ni_{4.2}Co_{0.3}Mn_{0.4}Al_{0.3}$ alloy is 0.23 wt.%, analytical Mg content of the alloys prepared on 1 kg- and 10 kg-batch scale was 0.20 and 0.23 wt.%, respectively. In small-scale preparation of alloy, Mg is more easily volatilized because of larger specific surface area of melt. It seems that this Mg volatilization takes the alloy composition out of stoichiometry and lowers homogeneity of the alloy.

Figs. 5 and 6 show high rate capability and cyclic behavior of test cells using the alloys with slightly increased Co content, $Mm_{1-x}Mg_xNi_{4.175}Co_yMn_{0.4}Al_{0.3}$ ($x = 0.04$, 0.05, and 0.06; $y = 0.325$), compared with that using the alloy with $y = 0.3$, respectively. By increasing the Co content from $y = 0.3$ to 0.325, cycle life of the alloys with $x = 0.04$ were significantly increased from 223 to 425 cycles, not changing the high rate capability. For the alloys with the Co content of $y = 0.325$, discharge capacity at the 10*C* rate and cycle life at the 1*C*/1*C* cycle test had the maximum value at $x = 0.05$. In terms of total electrode performance, the following alloy

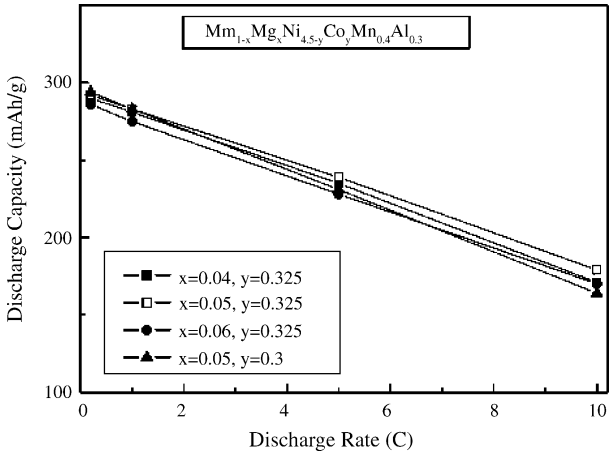

Fig. 5. Discharge capability vs. discharge rate of test cells using $Mm_{1-x}Mg_xNi_{4.5-y}Co_y Mn_{0.4}Al_{0.3}$ ($x = 0.04$, 0.05, and 0.06; $y = 0.3$ and 0.325) alloy electrodes at 25 °C.

composition, $Mm_{0.95}Mg_{0.05}Ni_{4.175}Co_{0.325}Mn_{0.4}Al_{0.3}$, was selected.

3.2. Effect of stoichiometric composition on the electrode properties

The Mg-added alloy with non-stoichiometric composition of B/A = 5.2 was investigated in the previous section. Detailed effect of stoichiometric composition on the electrode properties was studied. Lattice parameters and PCT results of the $Mm_{0.96}Mg_{0.04}Ni_zCo_{0.3}Mn_{0.4}Al_{0.3}$ ($z = 4.0$, 4.1, and 4.2) alloys with B/A ratio of 5.0, 5.1, and 5.2 are shown in Table 2. With increasing of the B/A ratio from 5.0 to 5.2, the lattice constant in *c*-axis was almost unchanged, the lattice constant in *a*-axis decreased from 5.043 to 5.029 Å, and then unit cell volume also decreased from 89.31 to 88.82 $Å^3$. Fig. 7 shows PCT curves for the alloys at 80 °C. With increasing the B/A ratio, the hydrogen storage capacity (H/M value) decreased, and the plateau pressure increased.

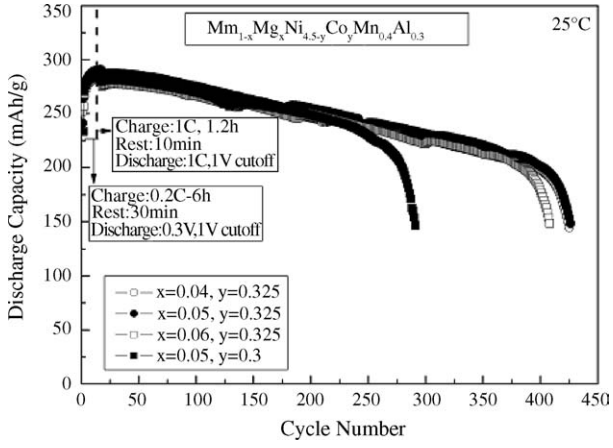

Fig. 6. Discharge capacity vs. cycle number in 1*C*/1*C* cycle test of test cells using $Mm_{1-x}Mg_xNi_{4.5-y}Co_yMn_{0.4}Al_{0.3}$ ($x = 0.04$, 0.05, and 0.06; $y = 0.3$ and 0.325) alloy electrodes at 25 °C.

Table 2
Lattice parameters and PCT results (80 °C) for $Mm_{0.96}Mg_{0.04}Ni_zCo_{0.3}Mn_{0.4}Al_{0.3}$ (z = 4.0, 4.1, and 4.2) alloys

z	Composition	Lattice constants		Unit cell volume (Å^3)	Plateau pressure (MPa)	H/M
		a (Å)	c (Å)			
4.0	$Mm_{0.96}Mg_{0.04}Ni_{4.0}Co_{0.3}Mn_{0.4}Al_{0.3}$	5.044	4.057	89.41	0.08	0.73
4.1	$Mm_{0.96}Mg_{0.04}Ni_{4.1}Co_{0.3}Mn_{0.4}Al_{0.3}$	5.036	4.061	89.18	0.11	0.73
4.2	$Mm_{0.96}Mg_{0.04}Ni_{4.2}Co_{0.3}Mn_{0.4}Al_{0.3}$	5.034	4.061	89.14	0.15	0.64

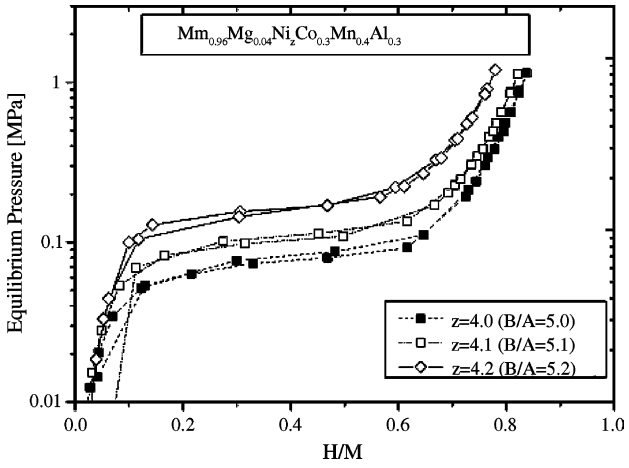

Fig. 7. PCT isotherms for $Mm_{0.96}Mg_{0.04}Ni_zCo_{0.3}Mn_{0.4}Al_{0.3}$ (z = 4.0, 4.1, and 4.2) alloys at 80 °C.

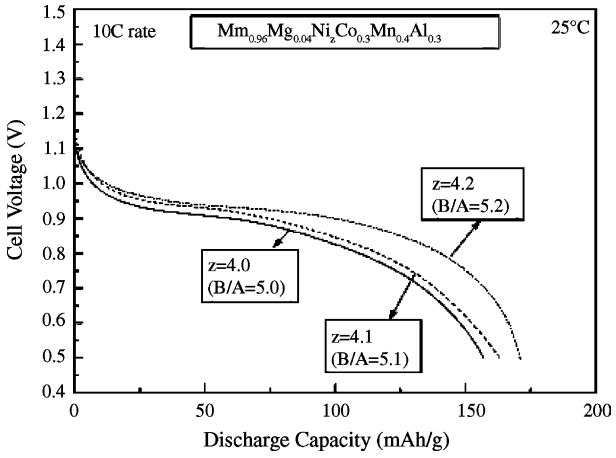

Fig. 8. Discharge curves of test cells using $Mm_{0.96}Mg_{0.04}Ni_zCo_{0.3}Mn_{0.4}Al_{0.3}$ (z = 4.0, 4.1, and 4.2) alloy electrodes at 10C rate (25 °C).

Fig. 8 shows discharge curves of test cells using $Mm_{0.96}Mg_{0.04}Ni_zCo_{0.3}Mn_{0.4}Al_{0.3}$ alloys at the 10C rate. The non-stoichiometric alloy with B/A = 5.2 had the lower theoretical capacity based on the PCT curve and higher plateau pressure than the alloy with B/A = 5.0, but showed higher discharge capacity at 10C rate.

Fig. 9 shows the result of TEM observation of the $Mm_{0.96}Mg_{0.04}Ni_{4.2}Co_{0.3}Mn_{0.4}Al_{0.3}$ alloy after 150 cycles of the 1C/1C cycle test. It was observed that many cracks were formed, and nickel was enriched on surface of the alloy. The Ni content increased from the bulk (66 at.%) to the surface (88 at.%), suggesting that excess Ni tends to segregate on the surface. This Ni segregation was observed only for the alloy after charge–discharge test. The increased high rate capability would be ascribed to the formation of this Ni-enriched layer as an electrocatalyst. It was ascertained that the over-stoichiometric alloy was suitable for high power use such as HEV application.

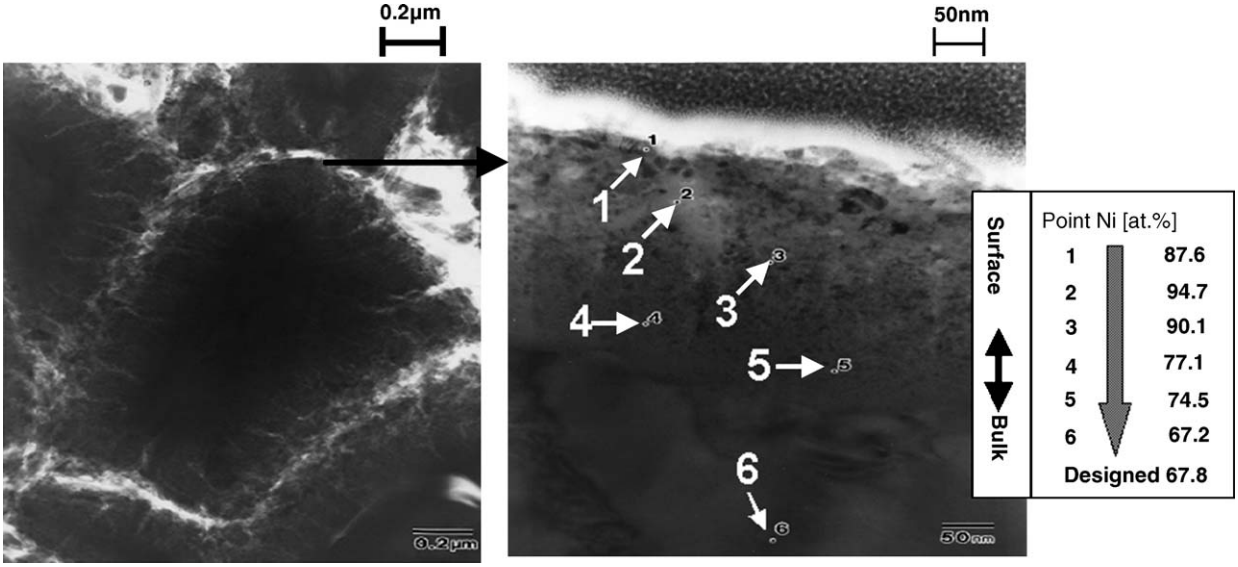

Fig. 9. TEM images and result of Mg determination of $Mm_{0.96}Mg_{0.04}Ni_{4.2}Co_{0.3}Mn_{0.4}Al_{0.3}$ alloy after 150 cycles of 1C/1C cycle test using test cell.

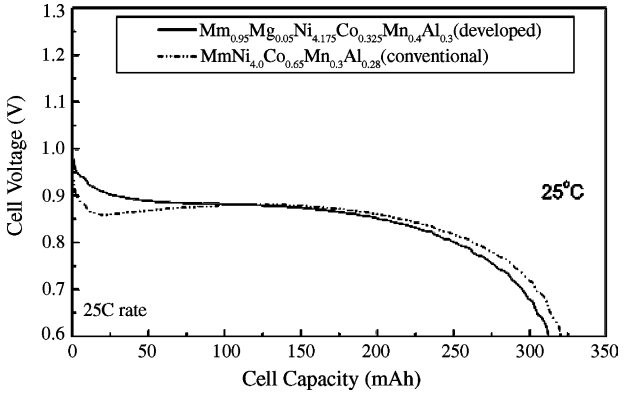

Fig. 10. Discharge curves of AAA-sized sealed cells using $Mm_{0.96}Mg_{0.04}Ni_{4.2}Co_{0.3}Mn_{0.4}Al_{0.3}$ alloy and the conventional alloy ($MmNi_{4.0}Co_{0.65}Mn_{0.3}Al_{0.28}$) electrodes at 25*C* rate (25 °C).

3.3. High rate capability and cycle life on sealed cell

The AAA-sized sealed cell was prepared using the developed alloy ($Mg_{0.96}Mg_{0.04}Ni_{4.2}Co_{0.3}Mn_{0.4}Al_{0.3}$) and its electrochemical properties were compared with that using the conventional alloy ($MmNi_{4.0}C_{0.65}Mn_{0.3}Al_{0.28}$). Fig. 10 shows discharge curves of the cells at the 25*C* rate. The cell using the developed alloy showed about 60 mV higher voltage than that using the conventional alloy in the initial stage of discharging, and showed comparable discharge capacity. Fig. 11 shows cycle behavior of the cells at 25 °C. At the 2*C*/2*C* cycling, the cell using the developed alloy showed only 10% of capacity decay ratio after 700 cycles, which was comparable to that using the conventional alloy. It is clear that the developed alloy had almost comparable high rate capability and cycle life as the conventional alloy in the sealed cell.

Finally, the developed alloy was tested using HEV mode cycle pattern (Fig. 1) at 45 °C on short-D-sized sealed cell. Fig. 12 shows the result of the HEV mode cycle test. The cell maintained 98% of initial capacity and 85% of initial power output even after 25,000 cycles, which is corresponding to travel of 100,000 km. It was concluded that the developed alloy would be used for HEV applications.

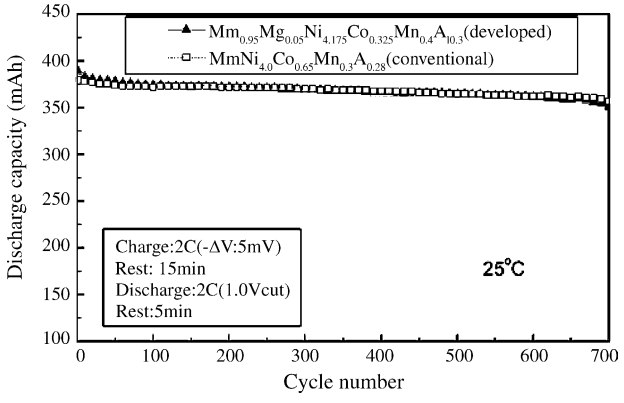

Fig. 11. Discharge capacity vs. cycle number in 2*C*/2*C* cycle test of AAA-sized sealed cells using $Mm_{0.96}Mg_{0.04}Ni_{4.2}Co_{0.3}Mn_{0.4}Al_{0.3}$ alloy and the conventional alloy ($MmNi_{4.0}Co_{0.65}Mn_{0.3}Al_{0.28}$) electrodes at 25 °C.

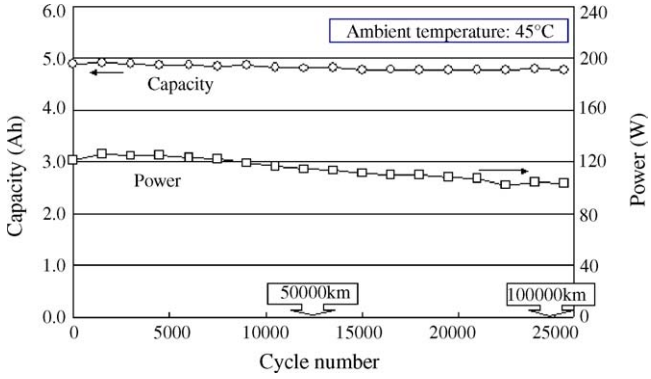

Fig. 12. Discharge capacity and power output vs. cycle number in HEV mode cycle test of short-D-sized sealed cell using $Mm_{0.95}Mg_{0.05}Ni_{4.175}Co_{0.325}Mn_{0.4}Al_{0.3}$ alloy electrode at 45 °C.

4. Conclusion

Mg-added alloy with low Co content was successfully developed satisfying both high rate capability and long cycle life. High rate capability of the $Mg_{0.96}Mg_{0.04}Ni_{4.175}Co_{0.325}Mn_{0.4}Al_{0.3}$ alloy was significantly improved by scaling up of alloy preparation batch from 1 to 10 kg. The reason is not clear at present, but it may be ascribed to their homogeneity. Overstoichiometric alloy with Ni-rich composition had lower theoretical capacity than stoichiometric alloy, but showed higher discharge capacity at the 10*C* rate, suggesting that the Ni-rich alloy is suitable for high power use. The developed alloy ($Mm_{0.95}Mg_{0.05}Ni_{4.175}Co_{0.325}Mn_{0.4}Al_{0.3}$) was finally tested using the HEV mode cycle pattern in short-D-sized sealed cell, showing more than 25,000 cycles of cycle life (travel of 100,000 km). It was demonstrated that the Mg-added low-Co alloy would be used for HEV application.

Acknowledgments

This work was performed under project (Strategic R&Ds on Rationalization technology for Use of energy and Innovative R&Ds on Fundamental Technology for Effective Utilization of Energy) supported by NEDO (The New Energy and Industrial Technology Development Organization).

References

[1] R.F. Nelson, J. Power Sources 91 (2000) 2–26.
[2] A. Taniguchi, N. Fujioka, M. Ikoma, A. Ohta, J. Power Sources 100 (2001) 117–124.
[3] M.L. Soria, J. Chacon, J.C. Hernandez, J. Power Sources 102 (2001) 97–104.
[4] J.J.G. Willems, Philips J. Res. 39 (1984) 1–5.

[5] T. Sakai, M. Matsumoto, C. Iwakura, in: K.A. Gschneidner Jr., L. Eyring (Eds.), Handbook on the Physics and Chemistry of Rare Earths, vol. 21, Elsevier, Amsterdam, 1995, pp. 133–178, and references cited therein.
[6] T. Sakai, H. Miyamura, N. Kuriyama, A. Kato, K. Oguro, H. Ishikawa, J. Electrochem. Soc. 137 (1990) 795–799.
[7] K. Hasegawa, H. Mori, M. Oshitani, Yuasa-Jiho (71) (1991) 13–19 (in Japanese).
[8] F. Meli, A. Züttel, L. Schlapbach, Z. Phys. Chem. Neue Folge 183 (1994) 371–377.
[9] B.V. Ratnakumar, C. Witham, R.C. Bowman, A. Hightower, B. Fultz, J. Electrochem. Soc. 143 (1996) 2578–2584.
[10] T. Sakai, H. Yoshinaga, H. Miyamura, N. Kuriyama, H. Ishikawa, J. Alloys Compd. 180 (1992) 37–54.
[11] P.H.L. Notten, R.E.F. Einerhand, J.L.C. Daams, J. Alloys Compd. 210 (1994) 221–232.
[12] F. Lichtenberg, U. Kohler, A. Folzer, N.J.E. Adkins, A. Züttel, J. Alloys Compd. 253 (1997) 570–573.
[13] W.-K. Hu, H. Lee, D.-M. Kim, S.-W. Jeon, J.-Y. Lee, J. Alloys Compd. 268 (1998) 261–265.
[14] C. Iwakura, K. Ohkawa, H. Senoh, H. Inoue, Electrochim. Acta 46 (2001) 4383–4388.
[15] K. Kadir, T. Sakai, I. Uehara, J. Alloys Compd. 257 (1997) 115–121.
[16] K. Kadir, T. Sakai, I. Uehara, J. Alloys Compd. 287 (1997) 264–270.
[17] T. Kohno, H. Yoshida, F. Kawashima, T. Inaba, I. Sakai, M. Yamamoto, M. Kanda, J. Alloys Compd. 311 (2000) L5–L7.
[18] T. Maeda, N. Shinya, S. Shima, Rare Earths 36 (2000) 220–221 (in Japanese).
[19] H.B. Yang, T. Sakai, T. Iwaki, S. Tanase, H. Fukunaga, J. Electrochem. Soc. 150 (2003) A1684–A1688.
[20] H.B. Yang, H. Fukunaga, T. Ozaki, T. Iwaki, S. Tanase, T. Sakai, J. Power Sources 133 (2004) 286–292.
[21] H. Fukunaga, M. Kishimi, N. Matsumoto, T. Ozaki, T. Sakai, T. Kishimoto, T. Tanaka, Electrochemistry 73 (2005) 31–37.
[22] Japan Automobile Research Institute Standards Committee, Cycle life test procedure of sealed nickel–metal hydride batteries for hybrid electric vehicles, JEVS D 716, Japan Automobile Research Institute, Tokyo, 2004.